M&C 2017 - International Conference on Mathematics & Computational Methods Applied to Nuclear Science & Engineering, Jeju, Korea, April 16-20, 2017, on USB (2017)

Development of a Coupled Neutron / Photon Transport Mode in the Serpent 2 Monte Carlo Code

Jaakko Leppänen*, Toni Kaltiaisenaho*, Ville Valtavirta*, Martti Metsälä†

**VTT Technical Research Centre of Finland, Ltd., P.O Box 1000, FI-02044 VTT, Finland*
†Aalto University, P.O Box 15100, FI-00076 AALTO, Finland
Jaakko.Leppanen@vtt.fi

Abstract - *This paper presents the early development of a coupled neutron / photon transport mode in the Serpent 2 Monte Carlo code. The methodology covers the production of prompt secondary gammas emitted in neutron interactions, using the ENDF reaction sampling laws in ACE format cross section libraries. The new transport mode is developed mainly to account for the effect of gamma heating in multi-physics simulations. Other potential applications include radiation shielding and fusion neutronics. The work is still under way, and at the time of this writing the distributed version of Serpent 2 lacks the capability to transport both neutrons and secondary photons simultaneously. The methodology is instead tested and demonstrated by dividing the simulation in two parts, and the results are compared to reference MCNP calculations. The test cases include a simple broomstick problem for the comparison of photon emission spectra, and gamma flux and heating calculations in an infinite BWR fuel lattice.*

I. INTRODUCTION

Capability to perform high-fidelity coupled multi-physics simulations has been one of the top priorities in the development of the Serpent 2 Monte Carlo code for several years [1, 2]. The coupling scheme is based on a universal multi-physics interface, designed for passing state-point information from external solvers to Serpent, and power distributions in the opposite direction, all without modifications in the geometry input. The methodology relies on a rejection sampling scheme that allows the modeling of continuous density and temperature distributions [3], together with an on-the-fly treatment for material temperatures [4, 5]. The coupling is designed to work with thermal hydraulics, CFD and fuel performance codes in steady-state and dynamic mode, including sub-, super- and prompt super-critical states [6, 7].

One of the challenges related to coupled multi-physics simulations is the accurate modeling of energy deposition in fuel, coolant and structural materials. Even though the vast majority of energy is deposited at the fission site as the kinetic energy of fission fragments, neutrons and prompt fission gammas carry a non-negligible fraction away from the fuel. In addition, parasitic neutron capture reactions with positive Q-value must be accounted for in the energy balance. The energy released in (n,γ)-reactions constitutes several percent of the recoverable fission energy, and for the most part it is deposited in the materials in the form of gamma radiation. The non-fission components of energy deposition may become important especially in fast transients, in which the heat produced in fuel is conducted into the coolant with a considerable delay, but the contribution of fission neutrons and prompt fission and capture gammas is practically instantaneous.

Accounting for the effect of gamma heating in the heat deposition model requires a coupled neutron / photon transport mode, in which the prompt gammas produced in fission, capture and inelastic scattering reactions are included in the transport simulation. The photon physics routines were implemented in Serpent 2 in 2015 [8], and the work has since then continued to the production of secondary photons in neutron reactions. This paper presents the methodology, together with some preliminary results. The fully coupled transport mode is still under development, but the physics routines can already be tested by dividing the calculation into source generation and stand-alone photon transport simulations. The secondary photon production routine is verified by comparing the emission spectra to reference MCNP calculations. The coupled simulation mode is demonstrated by a steady-state BWR assembly calculation.

II. METHODS

The neutron physics model in Serpent is based on cross sections and ENDF reaction laws read from ACE format data libraries, which were originally developed for the MCNP code [9]. The same applies to the production of secondary photons in neutron reactions. The physics routines for photons include additional models and data, which for some parts differ from that in MCNP. The methodology is briefly described below.

1. Photon Physics Model in Serpent 2

The detailed photon physics model was first introduced in Serpent version 2.1.24, released in June 2015. The photon transport mode can be used for elements from Z = 1 to 98 over the energy range from 1 keV to 100 MeV. The four main photon interactions are included: Rayleigh scattering, Compton scattering, photoelectric effect, and electron-positron pair production. A thick-target bremsstrahlung (TTB) approximation is used for taking into account the bremsstrahlung emitted by electrons and positrons. Secondary particles are also created through atomic relaxation in the form of fluorescence photons and Auger electrons.

Cross sections determining the reaction probabilities of photon interactions are obtained from ACE format libraries, but the models used for intraction physics requires additional data provided in auxiliary files. Most of this interaction data is derived from ENDF/B-VII.1, but also other sources are used.

A brief description of the physics models is provided below, and the details can be found in Ref. [8].

Rayleigh scattering, in which the direction of the photon is changed but the energy is unaltered, is modeled using the form factor approximation, which modifies the classically predicted Thomson scattering cross section. In Compton scattering, the direction and the energy of the photon are changed, and an electron is ejected from the atom. The direction of the Compton-scattered photon is sampled using the incoherent scattering function approximation, which modifies the free-electron Klein–Nishina cross section. The photon energy is sampled using the relativistic impulse approximation [10] which takes into account the Doppler broadening caused by momentum distributions of atomic electrons.

In photoelectric effect, the photon is absorbed and a photoelectron is emitted from the atom. The electron shell is selected with a probability given by the ratio of the shell cross section to the total photoelectric cross section. All shells (including sub-shells) with binding energies above 1 keV are included.

Pair production creates an electron-positron pair. The energy of the pair is sampled using the differential cross section given by Davies, Bethe and Maximon [11], together with screening functions by Butcher and Messel [12] and a low-energy correction factor used in the PENELOPE code [13]. Positron annihilation is modeled at rest, which results in the emission of two photons, both with an energy equal to the electron rest mass.

The TTB approximation is used for all the electrons (including positrons) created in the interactions. Continuous slowing down approximation (CSDA) is applied which results in average energy and number distributions of bremsstrahlung photons. The CSDA distributions require collision and radiative stopping powers along with bremsstrahlung energy cross sections. Collision stopping powers are calculated with the Bethe's formula [14, 15], including the density effect correction solved using the Sternheimer's method [16]. Bremsstrahlung energy cross section data is applied from Ref. [17], and radiative stopping powers are calculated from the data. Positrons are taken into account separately with the Bethe's formula, and by applying a scaling factor [13] for the cross sections.

There are some known differences in the photon physics models of Serpent and MCNP6, particularly in the angular distribution of photo-electrons, Doppler broadening of Compton-scattered photons, and pair production energy distribution. These differences, however, are noticeable mainly in detailed comparisons, and they are expected to be insignificant in gamma heating calculations.

Some differences have also been observed in the bremsstrahlung production. Unfortunately, the TTB method used in MCNP has not been documented in detail, as far as the authors are aware of, but some related information can be obtained from the documentation of electron physics. The physics applied to positrons in MCNP is identical to electron physics, with the exception of positron annihilation, whereas the TTB model in Serpent treats electrons and positrons as two different particle types. Because positrons have lower radiative yield compared to electrons, the total radiative yield of the electron-positron pair created in a pair production event is lower in Serpent than in MCNP.

Preliminary comparisons between Serpent, MCNP6, PENELOPE, and theoretical CSDA results also imply that the fully CSDA-based TTB approximation implemented in Serpent underestimates the radiative yield, and that the TTB method used in MCNP6 performs better in comparison to detailed electron transport calculations. These differences are observed mainly in high-Z materials at electron energies of about 5 MeV and above. The effect of these differences on the calculations presented here are expected to be small because the source spectrum is primarily dominated by photons with energies below a few MeV.

2. Coupled Neutron / Photon Transport Mode

Secondary photons are produced in various neutron interactions involving transmutations and energy transitions in the nucleon structure. A typical example is the parasitic (n,γ)-reaction, in which the neutron is captured by the nucleus, and the short-lived compound state with excess energy decays via gamma emission. In ACE format neutron transport libraries the emission of secondary photons is described using photon production cross sections and associated energy and angular distributions. The distributions are provided separately for discrete and continuum reactions, and the sampling is handled according to ENDF reactions laws. The procedures implemented in Serpent corresponds to the expanded photon production method in MCNP [18].

The photon production routine is called after the target nuclide has been sampled for a collision. The number of emitted particles is given by the ratio of the photon production cross section to the nuclide total, truncated to the nearest integer value. An additional photon is added with the probability given by the remaining decimal fraction. An alternative to this analog production mode is the implicit mode, in which a predefined number of photons is always produced, but their statistical weights are adjusted in such way that the total production rate is preserved. The procedure continues by sampling the emission reaction for each emitted photon, with probabilities given by the partial production cross sections divided by the total. The selected reaction mode determines which distributions are used for sampling the energy and direction of the emitted particle. Both the analog and the implicit method were implemented in Serpent 2.

As mentioned above, the coupled calculation mode capable of modeling neutrons and photons simultaneously has not yet been completed, and the emitted photons are instead written as source points into a file, to be used in a second transport calculation. Even though this approach can be applied to testing and validation purposes, it is considered somewhat impractical for routine calculations. The work on the fully coupled mode is currently under way.

3. Heat Deposition Models in Serpent 2

Of the average ~200 MeV of binding energy released per fission, some 4% is lost to neutrinos, and the remaining part is divided between fission fragments, neutrons and prompt and delayed beta and gamma radiation. Most of the excess neutrons end up being captured, especially in large reactor cores, and the additional energy released in (n,γ) reactions is in the order of 5-10 MeV per fission. Accurate modeling of fission heating requires accounting for all prompt and delayed components, together with the different mechanisms of energy transfer, in particular energy deposited on-site by fission fragments, kinetic energy of neutrons lost to elastic and inelastic scattering, and energy absorbed by materials in the form of gamma radiation.

For most applications it is sufficient to apply an approximate model, in which all energy is deposited at the fission site, and the additional energy released in (n,γ) reactions is accounted for using an empirical correction factor. This is also the approach used in the default heating model in the Serpent code – the energy deposited per ^{235}U fission is assigned a fixed value (202.27 MeV by default), and the corresponding energies for other actinides are obtained by scaling this number by the ratio of the corresponding fission Q-values. This simplified model is typically used in single-assembly infinite lattice calculations performed, for example, for the purpose of spatial homogenization. When the geometry model is already based on an (unrealistic) approximation, applying a rigorous heat deposition model may not even lead to a better result.

The approximate model may no longer be the best choice in full-core geometries, especially when leakage contributes significantly to neutron loss. The differences between the approximate and rigorous approach are even more emphasized in time-dependent simulations, in which all prompt effects follow the changes in reactor operating conditions, while delayed effects fall behind. In the extreme case of prompt super-critical transients even the prompt effects are divided into different time scales. Heat deposited in the fuel is conducted through the cladding with a considerable delay, while neutrons and photons interacting with the coolant cause an instantaneous heating effect, which may be reflected in the response caused by physical feedbacks.

The energy deposition of photons and neutrons can be evaluated using analog or implicit methods. In analog estimators the energy deposited in scattering is calculated event-by-event, taking into account the energy lost to inelastic reactions and emission of secondary particles. The analog estimator for photons also accounts for energy cut-off and the production of electrons and positrons, which are currently handled using TTB and other approximate methods. The advantage of the analog approach is that the deposited energy is estimated as accurately as possible, within the limits of the underlying physics model. The drawback is the low efficiency in regions where interaction probabilities are low.

The implicit methods rely on conventional flux tallies multiplied by response functions that represent the average deposited energy per single interaction. The advantage of this approach is the higher efficiency, especially when the track-length estimator is used. There are, however, certain drawbacks, especially when it comes to photon interactions. The physics model applied for calculating the response function should correspond to the one used in the transport simulation, and differences in interaction data, simulation parameters or physics models may lead to inaccurate results.

The recommended approach for Serpent is to use the implicit estimator for neutrons and analog estimator for photons. The neutron heat deposition tally is based on total KERMA coefficients provided in the ACE format data files. The analog photon heat deposition tally is scored after each interaction in which energy is lost: photoelectric effect, Compton scattering and pair production. The deposited energy consists of three components:

1) The fraction of electron kinetic energy that is not emitted as bremsstrahlung, which is equal to the energy that the electron loses through collisions and radiative losses that are below a predefined cutoff value (1 keV by default).

2) The component arising from the vacancy created in a photoelectric or Compton event. In this case, the deposited energy is equal to the fraction of the energy of the initial vacant shell that is not emitted as fluorescence photons or bremsstrahlung by Auger electrons.

3) Contribution of energy cut-off, i.e. termination of the photon history when the energy falls below a predefined cutoff value.

The corresponding tallies in MCNP are the implicit F6 heating tally for neutrons and the analog *F8 tally for photons. There are certain issues related to the F6 tally of MCNP in photon transport mode. First, the F6 tally is not scored with secondary photons generated by the TTB approximation, which means that bremsstrahlung does not contribute to the heating estimated by the tally. The reason is that the electron energy is already included in the response function used by the F6 tally, and therefore, using the F6 tally with bremsstrahlung photons would result in double counting. A consequence of neglecting bremsstrahlung is that heating can be overestimated in material regions where high-energy electrons and positrons are primarily created, and underestimated far from these regions. The magnitude of this effect depends on the nature of the problem and often on the physical size of the tally. If the energy-dependent net current of bremsstrahlung photons over the surface of the tally volume is zero on average [1], the F6 tally can be expected to yield a reasonably good result, provided that the interaction data and physics options correspond to the response function of the F6 tally.

III. FIRST RESULTS

At the time of this writing the coupled neutron/photon transport mode was still missing the capability to include both particle types within the same transport simulation. All Serpent results presented below were instead obtained from separate runs, in which the photons produced in the neutron transport simulation were written in a file, which was then used as the source distribution for a second photon transport simulation. This methodology is available in the current distribution version of Serpent 2 (update 2.1.28), but should be considered an intermediate solution and used for testing purposes only.

[1] Transport of electrons and positrons is excluded in this context.

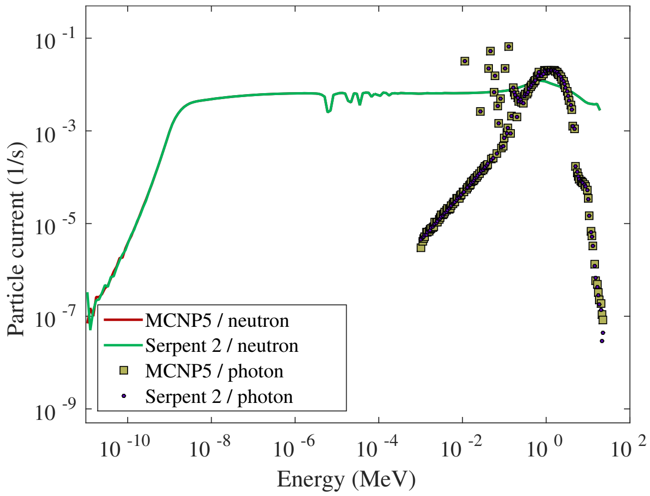

Fig. 1. Example of a "Broomstick" comparison calculation used for validating the photon production routine in Serpent 2 against MCNP5. Out-going neutron and photon current spectra calculated using the two codes. The example case is for ^{238}U from JENDL-4.0.

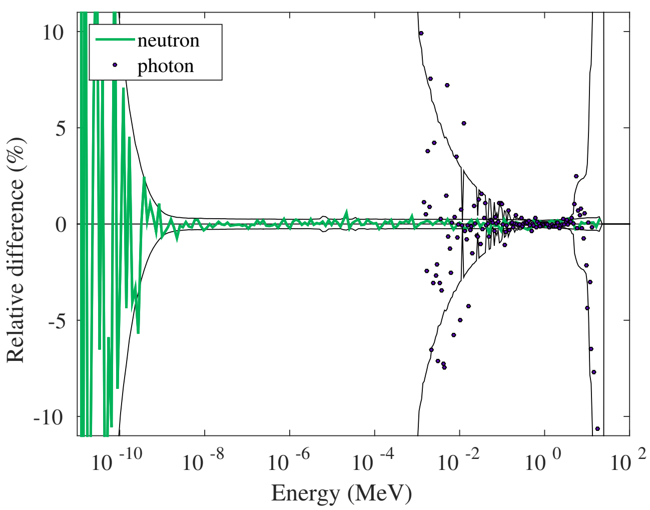

Fig. 2. Relative differences in the secondary neutron and photon spectra in Figure 1.

1. Validation of Secondary Photon Spectra

The production of secondary photons was validated by comparison to MCNP5 in a series of simple "Broomstick" calculations carried out for materials consisting of a single nuclide. The geometry consists of a narrow infinitely long cylinder, with a unidirectional neutron source. Secondary neutrons and photons produced in neutron reactions are deviated from the flight path, and they escape the cylinder before having the chance to interact for a second time. The direction and energy of the escaping particles is then captured using standard surface current tallies.

The broomstick test case can be considered ideal for validating the photon production model in Serpent, as any errors in the sampling routines are effectively isolated from other sources. The neutron physics routines in both Serpent and MCNP are based on the same ENDF reaction laws. Consistent results for neutrons verifies that any discrepancies in the photon emission spectra result from the production routine, instead of other factors, such as cross sections or unresolved resonance probability table sampling applied to neutron reactions. The fact that secondary photons have practically zero chance of interacting within the medium before escape rules out all discrepancies originating from the known differences in the photon physics models.

The comparisons were carried out for all nuclides included in the JEFF-3.2, ENDF/B-VII.1, JENDL-4.0 and FENDL-3.0 evaluated nuclear data files as part of an on-going project to produce new ACE format cross section libraries for Serpent 2. The work is still under way, but so far the consistency between the physics models used in MCNP and Serpent for the production of secondary prompt gammas has been confirmed. An example of such comparison is presented in Figures 1 and 2.

2. Prompt heating effects in BWR Assembly Calculation

The photon production routine and the direct heating effects of neutrons and prompt fission, capture and inelastic gammas was tested by comparison to MCNP6 in a study carried out at Aalto University during the Summer of 2016 [19]. The test case was a 2D infinite-lattice model of a single BWR fuel assembly. The transport calculation was run as a steady-state criticality source simulation. Even though the test case neglects neutron and photon leakage, as well as all delayed components of heat deposition, it can be considered a reasonable demonstration for the developed methodologies. Selected results are presented and discussed below.[2] The calculations were carried out using JEFF-3.2 based cross sections for neutrons and photon data from the eprdata12 library distributed with MCNP6. The implicit photon production mode was used in all calculations.

The secondary photon flux distribution calculated using Serpent was compared to a corresponding MCNP6 mesh tally in a 100 x 100 regular Cartesian mesh. The results are presented in Figures 3 and 4. The flux peaks in the region surrounding burnable absorber pins. This is explained by the fact that neutrons entering the gadolinium-doped fuel are absorbed in a very thin surface layer of the pellet, and the secondary photons emitted close to the surface have a higher probability of escaping in the surrounding medium. The differences between the codes remain between -0.7% and +0.4%, with a mean value of -0.13%. Even though the differences are small, they are not within the range of statistical uncertainty, which can be expected considering the small but non-negligible differences between the photon physics models. Even so, there appears to be no clear pattern in the way the differences are distributed in Fig. 4.

The comparison of photon heat deposition was performed using the *F8 tally in MCNP6 as the reference result. Instead of using a mesh tally the results were calculated for different

[2]The comparisons are focused on differerences between the codes. Running times and computational efficiency are considered irrelevant at this point because of the two-stage calculation scheme applied with Serpent.

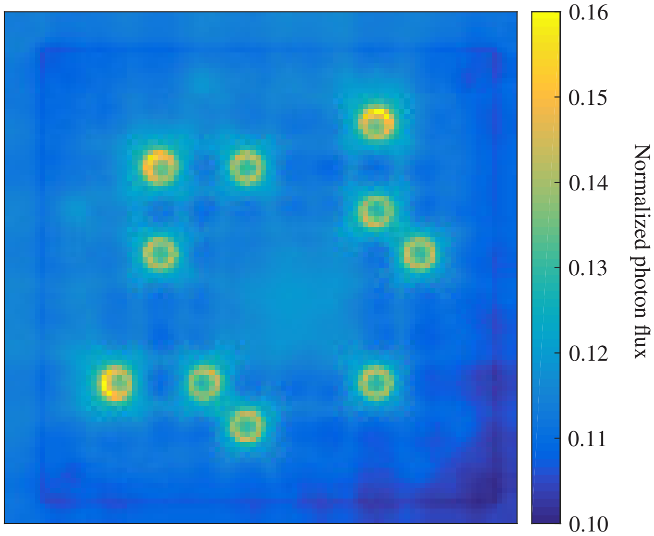

Fig. 3. Photon flux in the BWR fuel assembly calculated using Serpent 2. Normalized to a single source neutron.

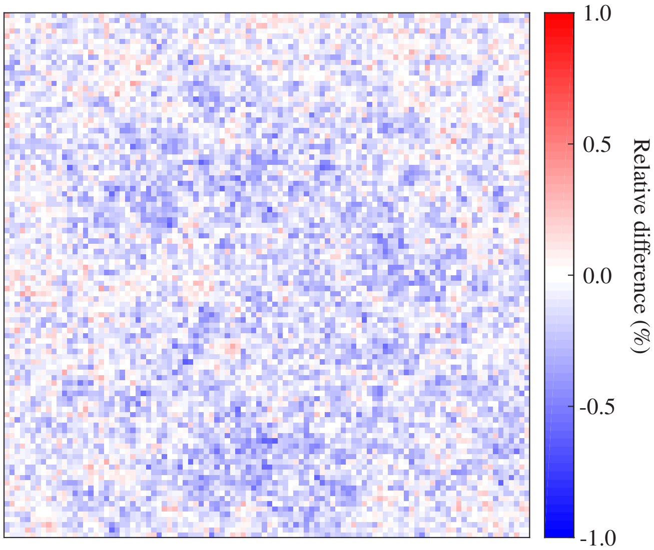

Fig. 4. Relative differences in photon flux between Serpent 2 and MCNP6.

material zones in the geometry. The comparison is presented in Table I. The highest values are obtained in the inner moderator channel wall and the lowest values in the moderator flowing outside the assemblies. The differences between Serpent 2 and MCNP6 are of similar order in magnitude as the differences in the flux distribution, which suggests that they most likely result from the same small differences in the photon physics model. Based on these results it appears that the photon heat deposition model in Serpent 2 works as expected.

IV. SUMMARY, DISCUSSION AND FUTURE PLANS

A coupled neutron / photon transport mode is being implemented in the Serpent 2 Monte Carlo code, mainly for the purpose of evaluating the contribution of direct photon heating in coupled multi-physics simulations. The development is still under way, but the first results involving a two-stage calculation scheme seem promising. The work continues by coupling the neutron and photon parts of the transport simulation into a single calculation mode. Once completed, the methodology provides the means to evaluate the prompt components of fission energy deposition in a rigorous manner. An accurate heat deposition model is considered important, for example, in the modeling of fast reactivity transients, in which the energy carried away by fission neutrons and prompt gammas is deposited in the coolant much faster than heat is conducted through the cladding.

Photons are also produced by radioactive decay, in which case their source rate follows changes in fission power with a considerable delay. Serpent already provides a source mode that combines material compositions to radioactive decay data read from ENDF format data files and forms the source distribution automatically, based on the isotopic emission spectra. The compositions of radioactive materials can be set up manually, or read from the output of a previous burnup or activation calculation. This methodology has been applied, for example, for the evaluation of shut-down dose rates in the ITER fusion reactor [20, 21]. The radioactive decay source mode could basically be used for providing the delayed component of gamma heating in steady-state calculations, in which the concentrations of short-lived radionuclides remain in equilibrium. Slow transients, however, require tracking the concentrations similar to delayed neutron precursors. Including the delayed effects in the heat deposition model is one of the topics for future work.

In addition to secondary photons produced in neutron interactions, there are also photonuclear reactions that produce secondary neutrons. Such reactions can be important, for example, for some CANDU reactor calculations, and the implementation of photonuclear physics has already been started. Even though Serpent was originally developed as a reactor physics code, there is some considerable on-going effort to expand the scope of applications to new fields, such as radiation transport and fusion neutronics. These applications also involve neutron transport problems in which the production of secondary gamma radiation plays a role. Development of a weight-window based variance reduction scheme [22] is a major part of this effort, and incorporating multiple particle types in the implicit simulation is considered a formidable challenge for future work.

V. ACKNOWLEDGMENTS

The work in this study was carried out in collaboration between VTT and Aalto University. The development of new calculation methods in Serpent 2 was funded from the KATVE project in the Finnish National Research Programme on Nuclear Power Plant Safety (SAFIR 2018).

REFERENCES

1. J. LEPPÄNEN, M. PUSA, T. VIITANEN, V. VALTAVIRTA, and T. KALTIAISENAHO, “The Serpent Monte Carlo code: Status, development and applications

TABLE I. Comparison of photon heat deposition calculated in a 2D BWR fuel assembly model using MCNP6 and Serpent 2. The MCNP results were calculated using the *F8 tally type and the Serpent results using response function -12. The values are normalized to a single neutron history, and statistical errors and relative differences between the codes given in percent.

Region	MCNP6	Serpent 2	Diff. (in %)
Fuel type 1 (1.8 wt-% ^{235}U)	6.9040E-02 (0.040)	6.9087E-02 (0.009)	0.068
Fuel type 2 (2.1 wt-% ^{235}U)	6.9341E-02 (0.020)	6.9409E-02 (0.005)	0.099
Fuel type 3 (2.6 wt-% ^{235}U)	7.0325E-02 (0.010)	7.0352E-02 (0.004)	0.038
Fuel type 4 (3.0 wt-% ^{235}U)	7.0087E-02 (0.030)	7.0136E-02 (0.007)	0.069
Fuel type 5 (3.4 wt-% ^{235}U)	7.2217E-02 (0.010)	7.2231E-02 (0.002)	0.019
Fuel type 6 (3.7 wt-% ^{235}U)	7.1217E-02 (0.010)	7.1234E-02 (0.001)	0.025
Fuel type 7 (3.7 wt-% ^{235}U + Gd)	8.9666E-02 (0.010)	8.9742E-02 (0.003)	0.084
Inner moderator channel wall	2.9158E-01 (0.010)	2.9142E-01 (0.003)	-0.055
Inner moderator channel water	1.0057E-02 (0.020)	1.0059E-02 (0.005)	0.018
Outer moderator channel wall	1.9523E-03 (0.050)	1.9524E-03 (0.011)	0.002
Outer moderator channel water	7.3641E-04 (0.040)	7.3564E-04 (0.010)	-0.104

in 2013," *Ann. Nucl. Energy*, **82**, 142–150 (2015).

2. J. LEPPÄNEN, V. HOVI, T. IKONEN, J. KURKI, M. PUSA, V. VALTAVIRTA, and T. VIITANEN, "The Numerical Multi-Physics project (NUMPS) at VTT Technical Research Centre of Finland," *Ann. Nucl. Energy*, **84**, 55–62 (2015).
3. J. LEPPÄNEN, "Modeling of Nonuniform Density Distributions in the Serpent 2 Monte Carlo Code," *Nucl. Sci. Eng.*, **174**, 318–325 (2013).
4. T. VIITANEN, "Development of a stochastic temperature treatment technique for Monte Carlo neutron tracking," D.Sc. Thesis, Aalto University (2015).
5. T. VIITANEN and J. LEPPÄNEN, "New Interpolation Capabilities for Thermal Scattering Data in Serpent 2," in "PHYSOR 2016," Sun Valley, ID, USA, May 1-5, 2016.
6. V. VALTAVIRTA, T. IKONEN, T. VIITANEN, and J. LEPPÄNEN, "Simulating Fast Transients with Fuel Behavior Feedback Using the Serpent 2 Monte Carlo Code," in "PHYSOR 2014," Kyoto, Japan, Sep. 28 - Oct. 3, 2014.
7. V. VALTAVIRTA, M. HESSAN, and J. LEPPÄNEN, "Delayed Neutron Emission Model for Time Dependent Simulations with the Serpent 2 Monte Carlo Code - First Results," in "PHYSOR 2016," Sun Valley, ID, USA, May 1-5, 2016.
8. T. KALTIAISENAHO, "Implementing a photon physics model in Serpent 2," M.Sc. Thesis, Aalto University (2016).
9. D. PELOWITZ (ED.), "MCNP6 User's Manual," LA-CP-13-00634, Los Alamos National Laboratory (2013).
10. R. RIBBERFORS, "Relationship of the relativistic Compton cross section to the momentum distribution of bound electron states," *Phys. Rev. B*, **12**, 2067–2074 (1975).
11. H. DAVIES, H. A. BETHE, and L. C. MAXIMON, "Theory of Bremsstrahlung and Pair Production. II. Integral Cross Section for Pair Production," *Phys. Rev.*, **93**, 788–795 (1954).
12. J. C. BUTCHER and H. MESSEL, "Electron number distribution in electron-photon showers in air and aluminium absorbers," *Nuclear Physics*, **20**, 15–128 (1960).
13. F. SALVAT, "PENELOPE-2014: A Code System for Monte Carlo Simulation of Electron and Photon Transport," Tech. rep., OECD-NEA, Issy-les-Moulineaux, France (2015).
14. H. BETHE, "Zur Theorie des Durchgangs schneller Korpuskularstrahlen durch Materie," *Annalen der Physik*, **397**, 325–400 (1930).
15. H. BETHE, "Bremsformel für Elektronen relativistischer Geschwindigkeit," *Zeitschrift für Physik*, **76**, *5*, 293–299 (1932).
16. R. M. STERNHEIMER, S. M. SELTZER, and M. J. BERGER, "Density effect for the ionization loss of charged particles in various substances," *Phys. Rev. B*, **26**, 6067–6076 (1982).
17. "Bremsstrahlung energy spectra from electrons with kinetic energy 1 keV–10 GeV incident on screened nuclei and orbital electrons of neutral atoms with Z = 1–100," *Atomic Data and Nuclear Data Tables*, **35**, 345–418 (1986).
18. X-5 MONTE CARLO TEAM, "MCNP – A General Monte Carlo N-Particle Transport Code, Version 5, Volume I: Overview and Theory," LA-UR-03-1987, Los Alamos National Laboratory (2003).
19. M. METSÄLÄ, "Accurate Heat Deposition Calculations in Nuclear Reactors Using Monte Carlo Neutron and Photon Transport," Special assignment, Aalto University (2016).
20. P. SIREN and J. LEPPÄNEN, "Expanding the Use of Serpent 2 to Fusion Applications: Development of a Plasma Neutron Source," in "PHYSOR 2016," Sun Valley, ID, May 1-6, 2016.
21. J. LEPPÄNEN and T. KALTIAISENAHO, "Expanding the Use of Serpent 2 to Fusion Applications: Shut-down Dose Rate Calculations," in "PHYSOR 2016," Sun Valley, ID, May 1-6, 2016.
22. J. LEPPÄNEN, T. VIITANEN, and O. HYVÖNEN, "Development of a Variance Reduction Scheme in the Serpent 2 Monte Carlo Code," in "M&C 2017," Jeju, Korea, Apr. 16-20, 2017.